Parameter Optimization of a Novel Contact Sensor Based on Frequency Response of 2-DOF Vibration Absorber System for Landmine Detection

Hussein F.M. Ali
Mechatronics and Robotics Eng. Dept., Innovation School, EJUST, Alex., Egypt. (Currently: Mechatronics Dept., Egyptian Academy for Engineering & Advanced Technology (EAE&AT)), Cairo, Egypt.
hussein.ali@ejust.edu.eg

Ahmed M. R. Fath El-Bab
Mechatronics and Robotics Eng. Dept., Innovation School, EJUST, Alex., Egypt; (On leave from Mechanical Eng., Dept. Faculty of Engineering, Assiut University, Egypt).
ahmed_rashad@yahoo.com

Zakarya Zyada, SM IEEE
Faculty of Engineering and Technology, Multimedia University, Jalan Ayer Keroh Lama, 75450 Melaka, Malaysia; (On leave from Mechanical Power Eng. Dept, Faculty of Eng, Tanta University, Tanta, Egypt)
zakarya.zyada@mmu.edu.my, zzyada@f-eng.tanta.edu.eg

Said M. Megahed
Mechanical Design and Production Engineering Dept., Faculty of Engineering, Cairo University, Giza, Egypt,
smegahed@ejust.edu.eg

***Abstract*— Unexploded Landmines, after wares, represent a serious problem, wastes life and money. Recent research states that contact sensors are promising. In this work, a novel contact sensor for landmine detection is presented. The sensor principle is based on the concept of 2-DOF vibration absorber system (two springs and two masses), to detect the presence of an object (landmine) in sand which is modeled as a third spring. The 3rd spring stiffness (the sand stiffness) can be measured as a function of the vibration absorber frequency ω_{Abs} (the frequency at which the 2nd mass gives minimum amplitude (theoretically proven: zero)) and the 1st mass gives amplitude near to peak. When the sand stiffness changes due to existence of the landmine, the vibration absorber frequency ω_{Abs} changes, and consequently the landmine can be detected. The mathematical proof of the idea is verified by simulation on Matlab and finite element COMSOL Multi-physics. The system parameters are chosen to be appropriate with the sand-landmine stiffness measurement range. The simulation results are optimized to give best sensitivity and linearity of the sensor output. The sensor gives sensitivity of 1559 Hz/(MN/m) and linearity better than 95%. Finally, a detailed design procedure for the contact stiffness sensor for landmine detection is developed.**

Keywords*— *Landmine detection, contact sensing, finite element, vibration, vibration absorber.

I. INTRODUCTION

Landmines impose a major danger on many regions in the world, because they increase the personal risk and restrict the development in such regions. There are more than 100 countries affected by Landmines, UneXploded Ordnances (UXO), and Explosive Remnants of War (ERW). Roughly, 20 countries are heavily-affected [1]. Landmine detection sensors are costive and dominant in the demining process and research [2]. Many sensing technologies and studies are opened. The most mature technologies are based on the electro-magnetic waves (like Electromagnetic induction metal detector (MD), magnometers, and Ground penetration radar (GPR)) [3].

The Humanitarian Demining Standards for clearance success must satisfy 99.6% to 200 mm depth (according to United Nation Department of Human Affairs (UNDHA)) and 100% (according to International Mine Action Standards (IMAS)). To satisfy high grad, until now, this relies on manual procedure (that uses 'prodding' or 'probing' excavation tool) [4]. This is why, Acoustic/Seismic and smart prodding are considered of the most promising technologies as they have Low false alarm, properties feedback [5].

Many concepts have been introduced based on contact Acoustic/Seismic sensor. Martin et al. [6, 7, 8] studied the elastic-wave interactions with landmines and investigated 2-DOF model of surface-contacting vibrometer. Ground excitation is based on remote source while the moving vibrometer measures the associated ground surface motion, which is affected by the buried landmine when exists.

Donskoy et al. [9, 10, 11, 12] studied the nonlinear response of the 2-DOF model of the soil-mine system. The perturbation method used in the model introduces for the derived analytical solution to describe both quadratic and cubic acoustic interactions at the soil-mine interface. This solution has been compared with actual field measurements to obtain the nonlinear parameters of the buried mines, which have been analyzed with respect to mine types and burial depths. It was found that the cubic nonlinearity could be a significant contributor to the nonlinear response. This effect has led to develop a new intermodulation detection algorithm based on dual-frequency excitation. Ishikawa and Iino [13] modeled an active sensing prodder and mine as 2-DOF model. The prodder emits white Gaussian noise vibration to identify the object in front of the pointed tip of the prodder by the frequency response and discrete Fourier transform. Muggleton et al. [14] explored point vibration measurements in order to detect shallow-buried objects. The ground itself is modeled as single DOF at low frequency. A shaker is used to excite the ground vertically and has a built in impedance head which senses both the applied force and the measured acceleration. They used the resonance frequency and acceleration to detect buried pipes. Parts critical fatigue effect may occur. Ali, et al. [15, 16] studied the ground surface pressure distribution changes when applying static load. The cases were buried objects (Anti-tank

landmine, Anti-personnel landmine, rock, and can) exist under the ground at depths and inclination angles. That indicates a clear change in the ground surface hardness and stiffness (around three times) especially at shallow objects.

In literature, the landmine problem and have been studied with numerous sensing technologies (MD, GPR, acoustic, seismic, etc.), and with various levels of complexity. One of these is based on the assumption that the ground/object is modeled as a spring [6, 7, 8]. Others modeled with nonlinear spring [12] and others with spring and damper [13, 14]. In our case, the dynamic study of the sand-landmine problem with the simplified assumption (Modeling the ground with just spring) is an initial step to extract the most clear and ideal relations and to prove the concept of the novel sensing method [17].

This paper is organized as follows: in section 2, based on the fact that the ground stiffness changes with the existence of a landmine, using the concept of 2-DOF vibration absorber, a novel stiffness sensor is modeled. In section 3, the measuring range of the sensor is selected to be compatible with the sand-landmine problem. In section 4, the parameters selection criterion is established. In section 5, a finite element model is developed to verify the sensor performance with the designed parameters using more than five different sets of parameters values. In section 6, based on the resultant sensitivity and linearity of each parameters set, the sensor parameters are optimized to give high sensitivity and linearity of the sensor output. Finally detailed design procedure is developed.

II. Sensor Model

A. System Description:

The sensor is modeled as 2-DOF system, where m_1, m_2, k_1, *and* k_2 are a small mass, a big mass, a low-stiffness spring and a high-stiffness spring, respectively. While the ground stiffness is modeled as k_o (object-stiffness to be sensed), as shown in Fig.1. The mass m_2 is subjected to sinusoidal excitation force: $f_u = F_u \sin(\omega t)$, where F_u is the excitation force amplitude and ω is the excitation frequency, respectively. The system is designed to satisfy the vibration absorber phenomenon where:

$$\omega_{11} = \sqrt{k_1/m_1} = \omega_{22} = \sqrt{k_2/m_2} \quad \cdots\cdots\cdots\cdots\cdots\cdots (1)$$

At k_o equals zero (no object is in contact) and when the system operates at $\omega = \omega_{22} = \omega_{11}$ the vibration absorber phenomenon occurred (where the displacement of the mass m_2 equals zero and the whole the excitation energy is absorbed by the mass m_1. where the absorber part (m_1, k_1) exerts a force equals and opposites to the acting force on m_2 [18]. When the sensor contacts an object with certain stiffness k_o, the overall system natural frequencies are shifted and also the vibration absorber frequency ω_{Abs} of the phenomenon is also shifted. There is a direct relation between k_o and that frequency as will be clarified in the following derivation.

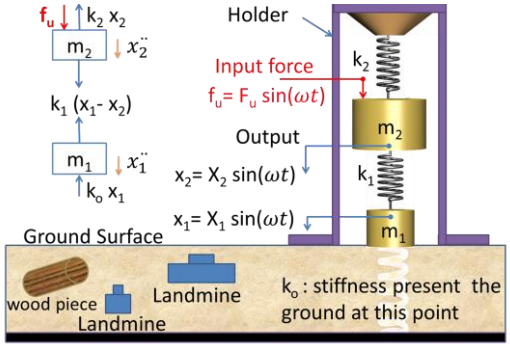

Fig.1. Sensor physical model and free body diagram.

B. Mathematical Derivation

From the free body diagram in Fig.1 the dynamic eq's are:

$$m_1 \ddot{x_1} + (k_o + k_1)\, x_1 - k_1 x_2 = 0 \quad \cdots\cdots\cdots\cdots\cdots\cdots\cdots\cdots (2)$$

$$m_2 \ddot{x_2} + (k_1 + k_2) x_2 - k_1 x_1 = f_u \quad \cdots\cdots\cdots\cdots\cdots\cdots\cdots\cdots (3)$$

By solving these differential eq's, the amplitudes X_1, X_2 are:

$$X_2 = \frac{\left[\frac{F_u}{k_2}\right]\left[\left(1+\frac{k_o}{k_1}\right) - \left(\frac{\omega}{\omega_{11}}\right)^2\right]}{\left[\left(1+\frac{k_1}{k_2}\right) - \left(\frac{\omega}{\omega_{22}}\right)^2\right]\left[\left(1+\frac{k_o}{k_1}\right) - \left(\frac{\omega}{\omega_{11}}\right)^2\right] - \frac{k_1}{k_2}} \quad \cdots (4)$$

$$X_1 = \frac{X_2}{\left[\left(1+\frac{k_o}{k_1}\right) - \left(\frac{\omega}{\omega_{11}}\right)^2\right]} = \frac{[F_u/k_2]}{\left[\left(1+\frac{k_1}{k_2}\right) - (\frac{\omega}{\omega_{22}})^2\right]\left[(1+\frac{k_o}{k_1}) - \left(\frac{\omega}{\omega_{11}}\right)^2\right] - \frac{k_1}{k_2}} \quad \cdots\cdots\cdots (5)$$

A vibration absorber phenomenon occurs at: $X_2 = 0$

$$\left[(1+\frac{k_o}{k_1}) - \left(\frac{\omega}{\omega_{11}}\right)^2\right] = 0 \quad \cdots\cdots\cdots\cdots\cdots\cdots\cdots\cdots\cdots\cdots (6)$$

$$X_1 = \frac{-F_u}{k_1} \quad \cdots\cdots\cdots\cdots\cdots\cdots\cdots\cdots\cdots\cdots\cdots\cdots (7)$$

Thus the frequency at the vibration absorber phenomenon:

$$\omega_{Abs} = \sqrt{\omega_{11}^2\left(1+\frac{k_o}{k_1}\right)} \quad \cdots\cdots\cdots\cdots\cdots\cdots\cdots\cdots\cdots\cdots (8)$$

Thus the ground stiffness k_o and the frequency (ω_{Abs}), at which the vibration absorber phenomenon occurs is as follows:

$$\boldsymbol{k_o = k_1\left(\frac{\omega_{Abs}^2}{\omega_{11}^2} - 1\right)} \quad \cdots\cdots\cdots\cdots\cdots\cdots\cdots\cdots\cdots\cdots (9)$$

III. Measuring Range of Sand-Landmine Problem

Unlike Young's modulus, static stiffness isn't only dependent on the material property of an object, but also on its dimensions. It is assumed that, the ground material is homogeneous elastic and incompressible (constant volume). If the ground is excited by a vertical load, f_u, acting over an indentor of radius r as shown in Fig. 2, the local static stiffness of the ground k_o can be expressed [19]:

$$E = \frac{(1-\nu^2)F}{2rd} \quad \cdots\cdots\cdots\cdots\cdots\cdots\cdots\cdots\cdots\cdots (10)$$

$$k_o = \frac{F}{d} = \frac{2rE}{(1-\nu^2)} \quad \cdots\cdots\cdots\cdots\cdots\cdots\cdots\cdots\cdots\cdots (11)$$

Where: E, ν, h, and d, are the Young's Modulus, Poisson's ratio of the ground, the ground height from rigid rock and indentation depth.

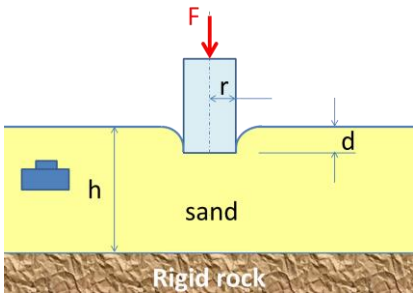

Fig.2. Indentation model parameters.

From Equation (11), in order to estimate the stiffness measuring range, it is required to select the Young's Modulus range and the indentor radius. From literature, typical medium uniform sand Young's modulus values: 30- 50 MPa [20], [21], [22], [23]. Based on the sand-landmine finite element model, the static stiffness of the ground above landmine increases around three times [15], [16]. In this model Young's Modulus range is selected to be up to 150 MPa (50MPa x 3) to represent the presence of landmine with the indentor radius of 5 mm. By applying Equation (11), the maximum static stiffness can be estimated to be 2 MN/m. On the other hand, the dynamic stiffness of ground above buried landmine could be as much as order of magnitude lower (depending on the excitation frequency and amplitude and burial depth) as compared to soil without buried mine [9]-[12]. And because that the proposed sensing concept correlates the stiffness to the excitation frequency at the vibration absorption mode, the target measuring range of the stiffness is estimated as 0-2 MN/m.

IV. Parameters Selection Criterion

In this section the sensor parameters (m_1, k_1, m_2, *and* k_2) selection is based on vibration absorber system as follows:

1. First of all the ratio between the springs' stiffnesses and the masses must satisfy the vibration absorber Eq. (1).
2. To get clear point of phenomenon occurrence (easily find zero displacement at m_2), $m_1/m_2 = 0.5$ is considered [18].
3. The relation between ω_{Abs}-k_o derived in Equations (8, 9), should be linear through the working range, in order to maintain constant sensitivity along the measuring range.
4. The sensitivity value ($d\omega_{Abs}/dk_o$), which is directly adapted by (k_1, and m_1) should be as large as possible to realize high accuracy when obtaining the object stiffness k_o.
5. The masses m_1 and m_2 should be as small as possible in order to not activate the landmine.
6. The masses m_1 and m_2 should be as small as possible in order to increase the frequency range at certain k_1, and k_2.

V. Modeling and Simulation

A. Mathematical Model:

In this section the frequency responses of x_1 and x_2, the displacements of the lumped masses m_1 and m_2, respectively, are determined using MATLAB, based on Equations (4, 5). Then, the frequency at which the zero displacement at m_2 occurs (vibration absorber phenomenon) is determined using the flowchart shown in Fig.3. The relation between the sand stiffness (k_o) and the corresponding frequency (ω_{Abs}), at which the vibration absorber occurs is determined as for the selected design parameters: m_1= 0.0017 kg, k_1= 1.78x10^3 N/m (based on the available Piezo actuator in Fig.4), m_2= 2 m_1, and k_2= 2k_1 (criteria 1 and 2 are applied here). Figure 4 shows the main element unit of piezoelectric transducer which is used to build the proposed stiffness sensor. The normalized displacements, of the two masses vs. the excitation frequency, are presented in Fig.5, at certain k_o values.

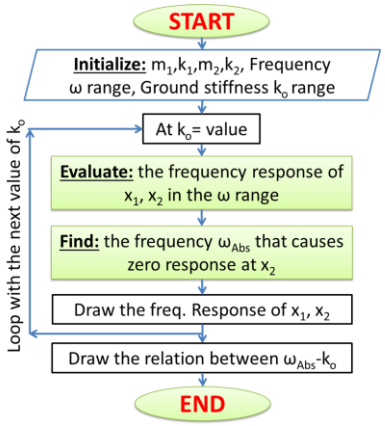

Fig.3. Flow chart of the mathematical model algorithm.

From the Fig.5.a, and at k_o= 0 N/m (blue curve), it is clear that the vibration absorber phenomenon happened at frequency $\omega = \omega_{Abs}$= 161.2 Hz, where the x_2 response equals zero. For the same sensor parameters but at different ground stiffness values: k_o= [10^4, 10^5] N/m, the corresponding vibration absorber frequencies are different. As presented in Fig.5.b, it is clear that this relation is nonlinear. This is why the sensor parameters should be properly selected to fulfill the criteria in section 4. In the next section a finite element method will be used to determine the vibration absorber frequency of the sensor system when subjected to different ground stiffness k_o, values. The sensor dimension will be selected to fulfill the selection criteria 3, 4, 5, and 6 in section 4.

B. Finite Element model (with COMSOL Multiphysics)

In this section the sensor parameters (m_1, k_1, m_2, *and* k_2) will be selected to give the best sensitivity and linearity of the sensor. The numerical values of the sensor parameters will be based on the commercial Piezo-electric actuators cantilever system as shown in Fig.6. The two springs k_1 and k_2, which are shown in Fig.1 are presented by the stiffness of the cantilever

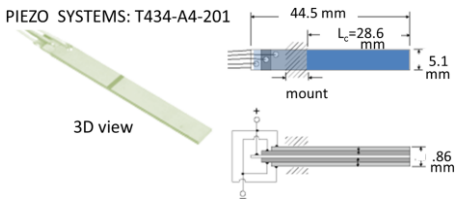

Fig.4. Piezo-Electric transducer (element unit) used to build the sensor

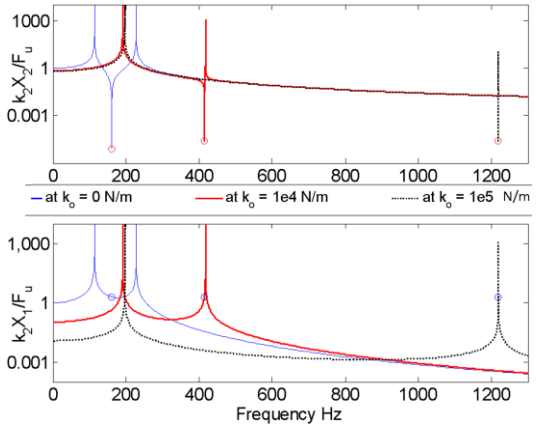

(a) x_2, x_1 frequency response

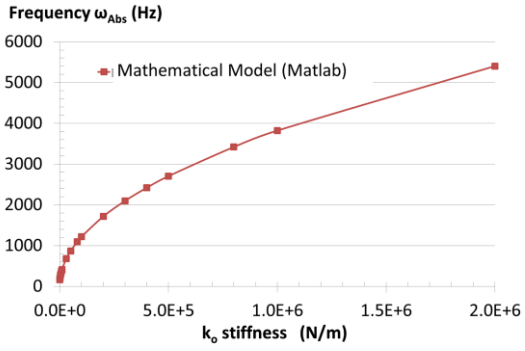

(b) Direct relation between ω_{Abs}-k_o

Fig.5. Frequency response at certain ground stiffness k_o values, and the corresponding vibration absorber frequency ω_{Abs}.

beams. The masses m_1 and m_2 of Fig.1 are represented by the equivalent masses of two Piezo-electric cantilever plus the concentrated masses as shown in Fig.6. The Piezo-electric actuator is chosen here because it offers excitation with high frequency range more than the frequency range offered by commercial motors used in the excitation systems, such as a rotating mass unbalance or a cam-follower.

The COMSOL model: *Model Type: 2D Solid Mechanics*

Material: Piezo-ceramic, Lead Zirconate Titanate, Piezo Systems Material Designation Type 5A4E (Navy Type II)
Elastic Modulus: 52 GPa, Poisson's: 0.38, Density: 8216 Kg/m^3

Geometry: As shown in Fig.7, the proposed sensor is modeled with two blocks for the two masses and two beams for the two springs k_1, and k_2, while the ground stiffness is modeled with k_o.
Beam1 width= Beam2 width=28.6 mm,
Mass1= 1.5 gm, Mass2= 3 gm.

Note: the mass m_1 in the mathematical modeling and MATLAB simulation is the equivalent mass [18]:

$$m_1 = Mass1 + \frac{beam1\ mass}{4} \quad \ldots\ldots\ldots\ldots\ldots\ldots\ldots\ldots\ldots (12)$$

Beam thickness (t) = n*0.86mm,

Where n = 1 to 5. This is to increase the beams stiffness dramatically based on the stiffness relation:

$$k = \frac{Ewt^3}{L_c^3} \quad \ldots\ldots\ldots\ldots\ldots\ldots\ldots\ldots\ldots\ldots\ldots\ldots\ldots\ldots\ldots (13)$$

Where: E, w, t, and L_c are the Young's Modulus, width, height, and length. Based on this relation and the n values, the stiffness k_1 is [1, 8, 27, 64, and 125] times the original spring stiffness with n=1 and t=0.86 mm. These values of k_1 will be used to study the effect of changing its value on the sensor sensitivity and linearity.

Solid Mechanics:

Boundary conditions: fixed from left.

Boundary load: applied at the end of the beam2, harmonic perturbation force per unit length in y direction: 5x10^2 N/m. **Note:** the width in y direction is 5.1 mm mean that force=2.6 N. Therefore the contact force applied to the ground during sensing will not exceed this value and it is very far from the activation force of the Anti-Personnel landmine (30 N) [16].

Variable stiffness spring is to represent the object stiffness

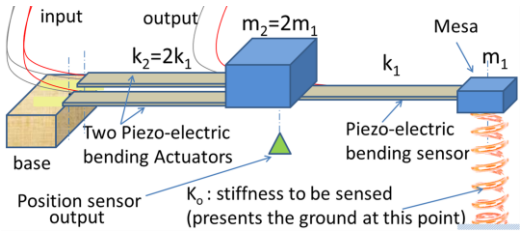

Fig.6. Piezo-electric version of the proposed sensor

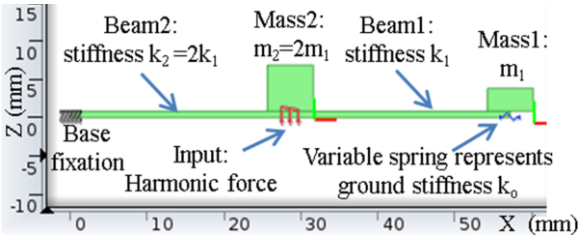

Fig.7. Finite element COMSOL model
2D beam model, load and boundary constrains

(the ground), at each beam thickness we will find the sensor output frequency with different ground stiff.: k_o= [0, 2] MN/m.

Meshing: Type: free Triangular. Size: extremely fine.

VI. Results and Parameter Optimization

In this section the two natural frequencies, the mode shapes, and the vibration absorber frequency of the system (composed of Piezo Systems: T434-A4-201), are determined.

A. Results:

The effect of changing the sand stiffness (k_o) on the sensor vibration absorber frequency is shown in Fig. 8 where the simulation results are presented for (n=1, k_1 =1.78 kN/m).

Figure 8 shows that, this design dimension couldn't satisfy the required measurement range 0- 2 MN/m because saturation occurs after stiffness (k_o) = 2x10^5 N/m. Also another problem appears that the vibration absorber frequency (ω_{Abs}) is very close to the upper natural frequency of the system in the range up to k_o = 10^5 N/m, as shown in Fig. 9. This means that it is difficult to distinguish the vibration absorber frequency (ω_{Abs}), during changing the excitation frequency. At k_o= 10^5 N/m the difference between the second natural frequency and the vibration absorber frequency is very small, around 14 Hz, which is one of the drawbacks of this design parameter value (n=1, k_1=1.78 kN/m).

B. Parameter Optimization

In this section may be better to start with a question: "How to maximize the linearity, range and also the sensitivity?" Fig. 8 shows the linearity in terms of square correlation (R^2) of the relation between ω_{Abs}-k_o in the range (0–2MN/m) at the design parameter (n=1, k_1=1.78 kN/m). R^2 =37% isn't acceptable.

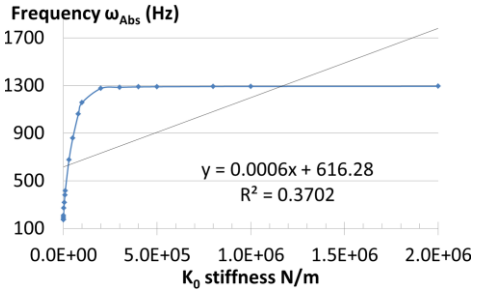

Fig.8. Linearity of the relation between ω_{Abs}-k_o (finite element model)
k_o range (0 – 2 MN/m) at (n = 1, k_1=1.78 kN/m).

The design criteria 1 and 2 is used with each design configuration at n= 1, 2, 3, 4, 5. For each stiffness k_1 in Table.1, finite element studies are carried out to find the vibration absorber frequency (ω_{Abs}) when the ground stiffness (k_o) changes in the range (0 – 2 MN/m). After that the

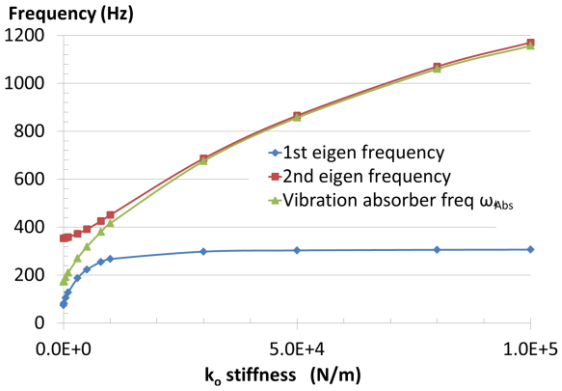

Fig.9. Sensor frequencies when changing stiffness k_o at (n=1, k_1=1.78 kN/m).

sensitivity and the linearity are calculated for each design configuration based on the selection criteria in section 4.2.

To find the best sensor stiffness k_1, the sensitivity and linearity is drawn vs. k_1, as shown in Fig.10. It shows also that the linearity increases as the stiffness k_1 increases. On the other hand the sensitivity increases also up to a certain level and then decreases. For getting best sensitivity with acceptable linearity, one of the three optimization rules are considered, as follows:

1. Select k_1 which give max sensitivity: at k_1= 6.5 x10^4 N/m Sensitivity=3200 Hz/ (2MN/m) =1600 Hz/ (MN/m) But linearity is not good: 91%
2. Or select the breakpoint, the best of both sensitivity and linearity (considering the importance of both is equally weighted): at k_1= 1.8x10^5 N/m, linearity= 95.1% and sensitivity= 3080 Hz /(2MN/m) = 1540 Hz /(MN/m)
3. Or select the best possible sensitivity that satisfy some acceptable linearity such as 95%, from the standard Piezo-electric actuator (n=4, k_1=1.14x10^5 N/m) linearity= 95% and sensitivity= 1559.38 Hz/ (MN/m)

By analyzing these optimization rules, and considering our target to fabricate a sensor with best performance. The 1st rule is not suitable as the linearity is not good, 91%. The 2nd rule doesn't enhance the linearity too much than the 3rd rule and also lower sensitivity. Based on the (n = 4) parameters configuration can be considered an optimum, at which: k_1=114 kN/m, k_2=2*k_1=228 kN/m.

According to the design criteria 5 and 6 (to minimize the masses as possible), m_2 is selected by adding the equivalent mass of the beam2 to the expected lumped mass (3gm) of a position sensor at mass2, as shown in Fig.6. m_2= 5 gm, m_1= *0.5* m_2 =2.5 gm.

After determining the best sensor parameter in the range of sand stiffness, the finite element simulation is carried out to examine these parameters on the sensor behavior.

Table 1. Parameter $k_1$changes effect on sensitivity and linearity

n	k_1 (a)	Total equivalent mass m_1 (a)	Sensitivity	R^2
	N/m	kg	Hz/(2MN/m)	
1	1.78x10^3	0.00173	1121.25	0.37
2	1.43x10^4	0.00199	2313.72	0.68
3	4.82x10^4	0.00224	3136.05	0.90
4	1.14x10^5	0.00250	3118.76	0.95
5	2.23x10^5	0.00275	2795.01	0.96

(a) m_1 and k_1 and are calculated based on Equations 12, and 13.

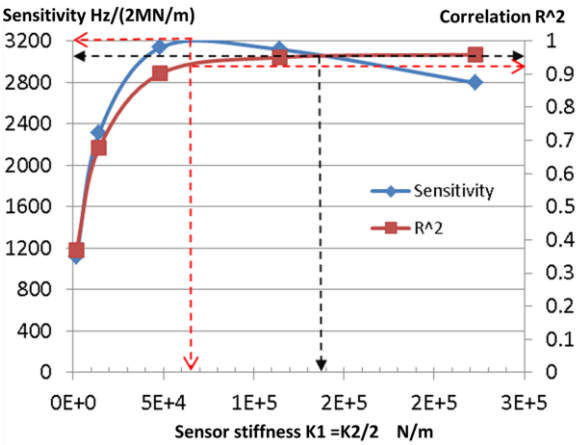

Fig.10. Optimization based on the sensor stiffness k_1.

C. Sensor Behavior with Optimum Parameter

This section will present simulation of the sensor with optimized parameters using the finite element by COMSOL, and then these results will be compared with the simplified mathematical model derived in section 2.2, using MATLAB.

The COMSOL model here is the same as that described in section 5.2, as shown in Fig.7, except that in **Geometry:** Height = 4*0.86mm. As n= 4, so the number of actuators at beam1 is four layers and hence k_1=1.14x10^5 N/m.

Figure 11 shows the vibration absorber frequency (ω_{Abs}), and the two natural frequencies of the sensor at different k_o. It is clear that the vibration absorber frequency (ω_{Abs}) can be easily distinguished from the two natural frequencies (the difference is more than 200 Hz in the worst case). The natural frequency mode shapes and the vibration absorber case of the sensor with optimum parameters are shown in Fig.12.

By applying the optimum parameters to the algorithm in Fig.4, the frequency response at the lumped masses m_1 and m_2 based on Equations 4, 5 can be calculated by MATLAB. Figure 13 shows a comparison between the mathematical results from MALAB and the finite element by COMSOL. As shown in Fig. 13 a very small difference 2-5% occurred between the mathematical calculation by MATLAB and finite

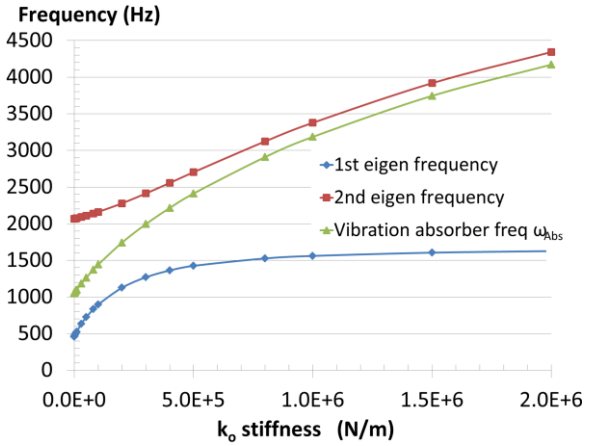

Fig.11. Optimum Sensor frequencies change when changing stiffness k_o Range (0-2 MN/m) at (n = 4, k_1=1.14x10^5 N/m).

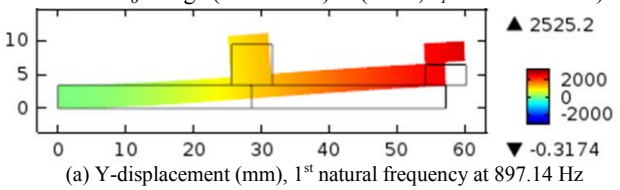

(a) Y-displacement (mm), 1st natural frequency at 897.14 Hz

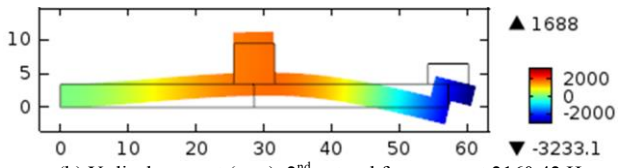

(b) Y-displacement (mm), 2nd natural frequency at 2160.42 Hz

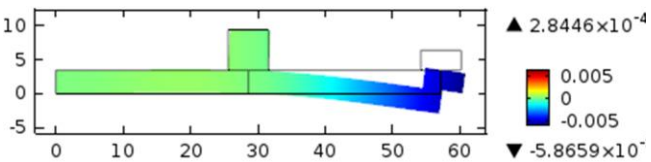

(c) Y-displacement (mm), Vibration absorber phenomenon at frequency ω_{Abs}=1441.16 Hz when displacement =0 at m_2.

Fig.12. finite element COMSOL model responses at ground stiffness k_o = 10^5 N/m and (n = 4 , k_1=1.14x10^5 N/m).

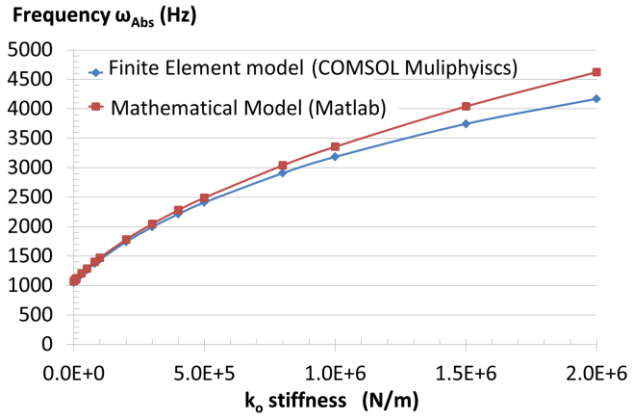

Fig.13. Optimum design comparison between the theoretical results and finite element results for stiffness k_o range (0 – 2 MN/m) at (n = 4, k_1=1.14x10^5 N/m).

element simulation by COMSOL.

VII. Design Procedure of the Sensor

This concept can be applied to any application in which the stiffness measurement is needed. The measurement range may be modified according to the application. Then the following design procedure can be applied to find the best sensitivity and linearity of the sensor in the desired range as follows:

1. Start with the selection of the measuring range according the required application, see section 3. For sand-landmine problem a range of (0 to 2 MN/m) is selected.
2. Decide the required masses at m_1 and m_2, which include some additional parts (ex: position sensor). It must be low, because increasing the masses decreases the sensitivity.
3. Use the simplified mathematical model to investigate the sensor performance Equation (9). As initial guess let k_1= one-twentieth max range of k_o.
4. If the sensor performance is good, in terms of linearity and sensitivity. Then the fine tuning can be done.
5. Use a finite element modeling tool, to verify the simplified mathematical model and to find the relation between the vibration absorber frequency ω_{Abs} and the sand stiffness k_o.
6. Find the sensitivity and linearity at each k_1.
7. Repeat 4, 5, and 6 at number of points around the correct guess of k_1. Then draw the sensitivity and linearity against k_1 (Fig.10). Then apply the suitable optimization rules: the best sensitivity with linearity measure R^2=95%, see section 6.2, to find the best sensitivity and linearity.

Acknowledgment

This research is funded by the Egypt-Japan University of Science and Technology (EJUST), Alexandria, Egypt.

References

[1] Said M. Megahed, Hussein F.M. Ali, and Ahmed H. Hussein: “Egypt Landmine Problem: History, Facts, Difficulties and Clearance Efforts”, International Symposium Humanitarian Demining, Šibenik, Croatia, (2010).

[2] Furuta, Katsuhisa; Ishikawa, Jun (Eds.): “Anti-personnel landmine detection for humanitarian demining”, springer (2009).

[3] “Detectors and Personal Protective Equipment Catalogue 2009”, GICHD: Geneva International Centre for Humanitarian Demining, Geneva, (2009).

[4] M.Habib: “Humanitarian Demining Innovative Solutions and the Challenges of Technology”,ARS Publisher, (2008).

[5] Macdonald, J., Lockwood, J.R., Mcfee, J., Altshuler, T., Broach, T., Carin, L., Harmon, R., Rappaport, C., Scott, W. and Weaber, R.: “Alternatives for Landmine Detection” (Pittsburg, PA: RAND), (2003).

[6] Waymond R. Scott Jr., James S. Martin, and Gregg D. Larson: “Experimental Model for a Seismic Landmine Detection System”, IEEE Transactions on Geoscience and Remote Sensing, vol. 39, no. 6,(2001).

[7] James S. Martin, Gregg D. Larson, and Waymond R. Scott Jr.: “Surface-Contacting Vibrometers for Seismic Landmine Detection”, Proc. of SPIE Vol. 5794, Bellingham, WA,(2005).

[8] James S. Martin, Gregg D. Larson, and Waymond R. Scott Jr.: “An investigation of surface-contacting sensors for the seismic detection of buried landmines”, J. Acoust. Soc. Am., Vol. 120, No. 5, (2006).

[9] D. M. Donskoy,A. Reznik, A. Zagrai, and A. Ekimov: “Nonlinear vibrations of buried landmines”, J. Acoust. Soc. Am. 117 (2), (2005).

[10] D. M. Donskoy: “Nonlinear vibro-acoustic technique for land mine detection”, SPIE's Proceedings on Detection and Remediation Technologies for Mines and Minelike Targets III, Vol. 3392, pp. 211-217, (1998).

[11] D. Donskoy, A. Ekimov, N. Sedunov, and M. Tsionskiy: “Nonlinear seismo-acoustic land mine detection and discrimination”, J. Acoust. Soc. Am. 111(6), 2705-2714, (2002).

[12] D. Donskoy, A. Ekimov, N. Sedunov, and M. Tsionskiy: “Nonlinear seismo-acoustic land mine detection: Field test”, SPIE's Proceedings on Detection and Remediation Technologies for Mines and Minelike Targets VII, Vol. 4742, pp. 685-695, (2002).

[13] Jun Ishikawa, and Atsushi Iino: “A Study on Prodding Detection of Antipersonnel Landmine Using Active Sensing Prodder”, International Symposium: Humanitarian Demining 2010, Šibenik, Croatia, (2010).

[14] J.M. Muggleton, M.J. Brennan, and C.D.F. Rogers: “Point vibration measurements for the detection of shallow-buried objects”, Tunnelling and Underground Space Technology (39) 27–33, (2014).

[15] Hussein F.M. Ali, Zakarya Zyada, Ahmed M. R. Fath El Bab, and Said M. Megahed: “Inclination Angle Effect on Landmine Characteristics Estimation in Sandy Desert using Neural Networks”, The 10th Asian Control Conference (ASCC 2015), (2015).

[16] Hussein F.M. Ali, Ahmed M. R. Fath El Bab, Zakarya Zyada, and Said M. Megahed "Estimation of Landmine Characteristics in Sandy Desert using Neural Networks", Journal of Neural Computing and Applications, Springer, (Accepted: Dec 21, 2015). DOI: 10.1007/s00521-015-2153-z

[17] Hussein F.M. Ali, Ahmed M. R. Fath El Bab, Zakarya Zyada, and Said M. Megahed "Novel Contact Sensor Concept and Prototype based on 2-DOF Vibration Absorber System", Intelligent Systems, Modelling and Simulation, IEEE 7th International Conference, ISMS 2016. DOI 10.1109/ISMS.2016.70

[18] W. T.Thomson:“Theory of Vibration with Applications”, Springer US,1993.

[19] J. W. Harding, I. N. Sneddon: “The elastic stresses produced by the indentation of the plane surface of a semi-infinite elastic solid by a rigid punch”, Mathematical Proceedings of the Cambridge Philosophical Society, Volume 41, Issue 01, pp.16-26, (1945)

[20] Obrzud R. and Truty A.: “The Hardening Soil Model - A Practical Guidebook”, Z Soil. PC 100701 report, revised 31.01.2012

[21] Kezdi, A.: “Handbook of Soil Mechanics”. Elsevier, Amsterdam, (1974).

[22] Prat, M., Bisch, E., Millard, A., Mestat, P., and Cabot, G. “La modelisation des ouvrages”. Hermes, Paris, (1995).

[23] Geotechdata.info, “Soil Young's modulus”, site: http://geotechdata.info /parameter/soil-elastic-young-modulus.html (09.2013), last check 09-2015.